Supporting Information

A Chicken Tapasin ortholog can chaperone empty HLA-B*37:01 molecules independent of other peptide-loading components

Georgia F. Papadaki[1,2], Claire H. Woodward[1,2], Michael C. Young[1,2], Trenton J. Winters[2], George M. Burslem[2,3] and Nikolaos G. Sgourakis[1,2,*]

[1]Center for Computational and Genomic Medicine, Department of Pathology and Laboratory Medicine, The Children's Hospital of Philadelphia, Philadelphia, PA, 19104, USA
[2]Department of Biochemistry and Biophysics, Perelman School of Medicine, University of Pennsylvania, 3401 Civic Center Blvd, Philadelphia, PA, 19104, USA
[3]Department of Cancer Biology and Epigenetics Institute, Perelman School of Medicine, University of Pennsylvania, Philadelphia, PA, 19104, USA

***Correspondence:**
Nikolaos G. Sgourakis
Nikolaos.Sgourakis@Pennmedicine.upenn.edu

This PDF file includes:

Figures S1 to S5

Table S1

Figures

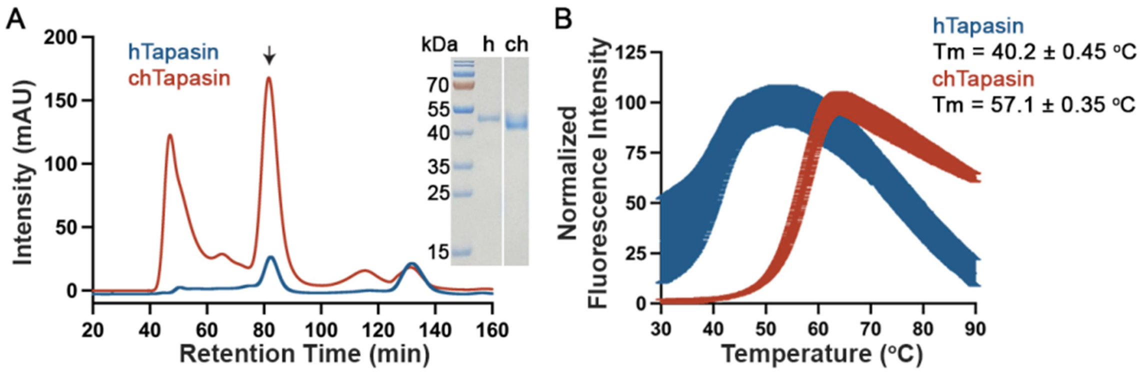

Figure S1. Chicken Tapasin can be expressed in high yields with improved stability. A. Size exclusion chromatography (SEC) traces of human (h) and chicken (ch) Tapasin proteins expressed in insect cells. The protein peaks are indicated by the arrow and were further validated by SDS-PAGE analysis. The additional peaks correspond to protein aggregates (40-70 min). **B.** Differential scanning fluorimetry (DSF) of human versus chicken Tapasin. Melting temperatures are in degrees Celsius (T_m). Data are mean ± SD obtained from n = 3 independent experiments.

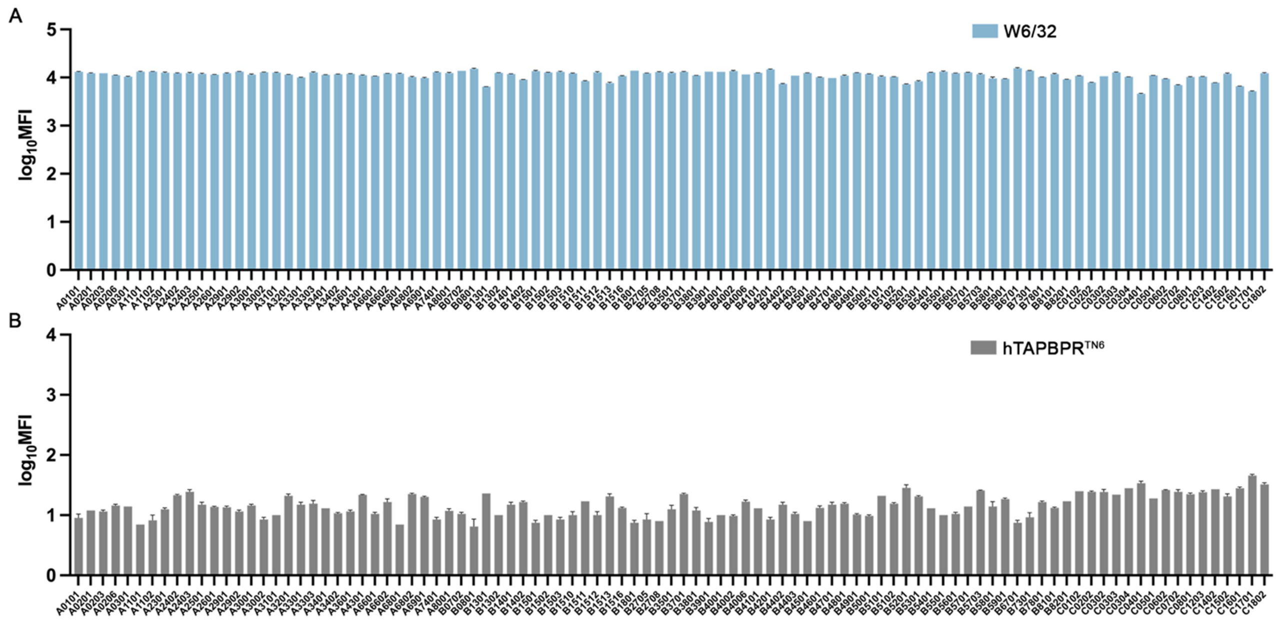

Figure S2. Binding levels of human and chicken Tapasin on HLA single antigen beads. A. Similar levels of peptide-loaded MHC-I molecules on the beads were observed upon staining with the primary anti-HLA class I antibody W6/32 conjugated with PE (Biolegend, 311406). **B.** Bar graph showing the binding levels of tetramerized hTAPBPR^{TN6} (negative control) to 97 different HLA allotypes on the SABs expressed as logarithm of Mean Fluorescence Intensity (MFI). The plotted data are mean ± SD of n = 3 independent experiments.

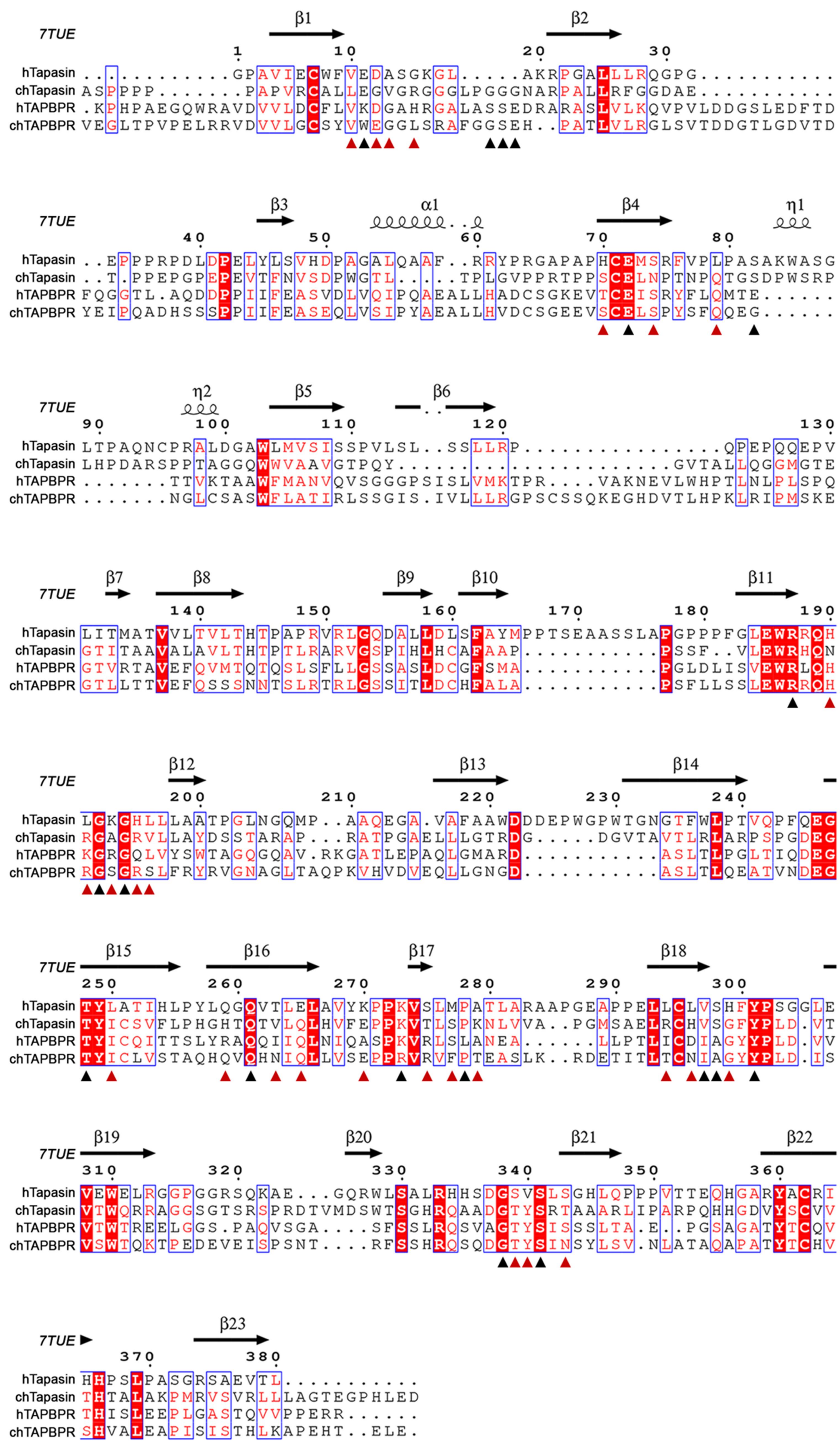
7TUE
β1
β2
β3
α1
β4
η1
η2
β5
β6
β7
β8
β9
β10
β11
β12
β13
β14
β15
β16
β17
β18
β19
β20
β21
β22
β23
hTapasin
chTapasin
hTAPBPR
chTAPBPR

Figure S3. Sequence alignment of human and chicken Tapasin and TAPBPR. Alignment of the luminal domains of human Tapasin (hTapasin; UniProt: O15533), chicken Tapasin (chTapasin; UniProt: A4F5A9), human TAPBPR (hTAPBPR; UniProt: Q9BX59), and chicken TAPBPR (chTAPBPR; NP_001382952.1). Conserved or polymorphic residues between human and chicken Tapasin on the interface with HLA-B*37:01 are shown in black or red, respectively. The secondary structure of human Tapasin (PDB ID: 7TUE) is provided as reference (1). Conserved residues are marked in blue boxes. Alignment was performed in ClustalOmega (2) and processed in ESPript (3).

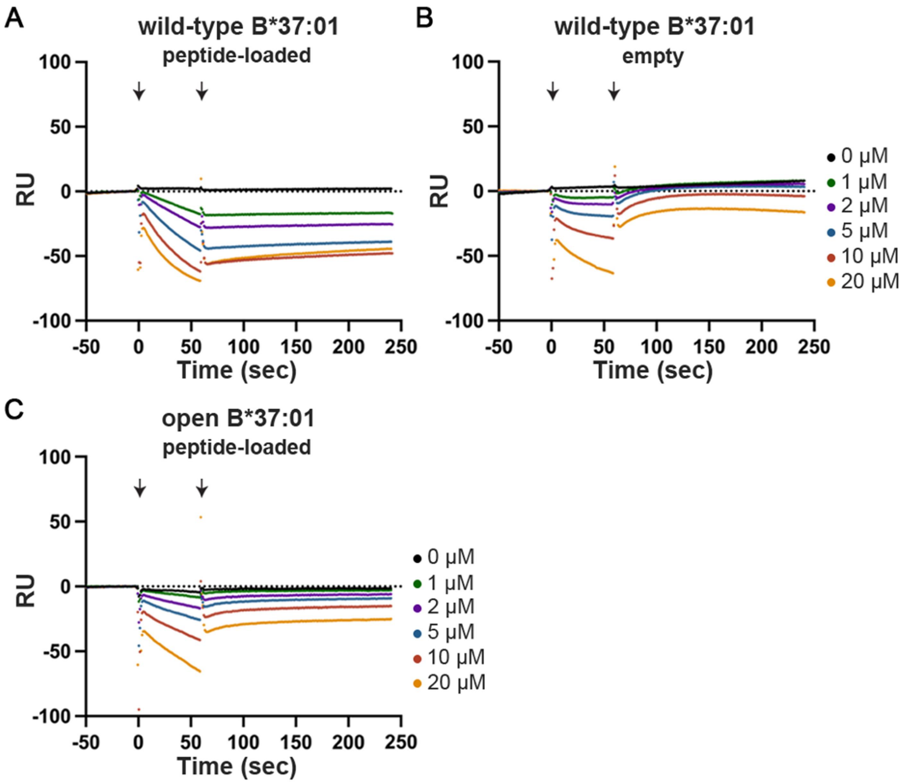

Figure S4. Chicken Tapasin interactions are restricted to the open, empty B*37:01. SPR sensorgrams of varying concentrations of soluble wild-type **A.** peptide-loaded, and **B.** -deficient B*37:01 or **C.** open, peptide-loaded B*37:01 flown over a streptavidin chip coupled with biotinylated chTapasin. Injection and washing start points are indicated by arrows. RU, resonance units. The plotted data are mean ± SD of n = 3 independent experiments.

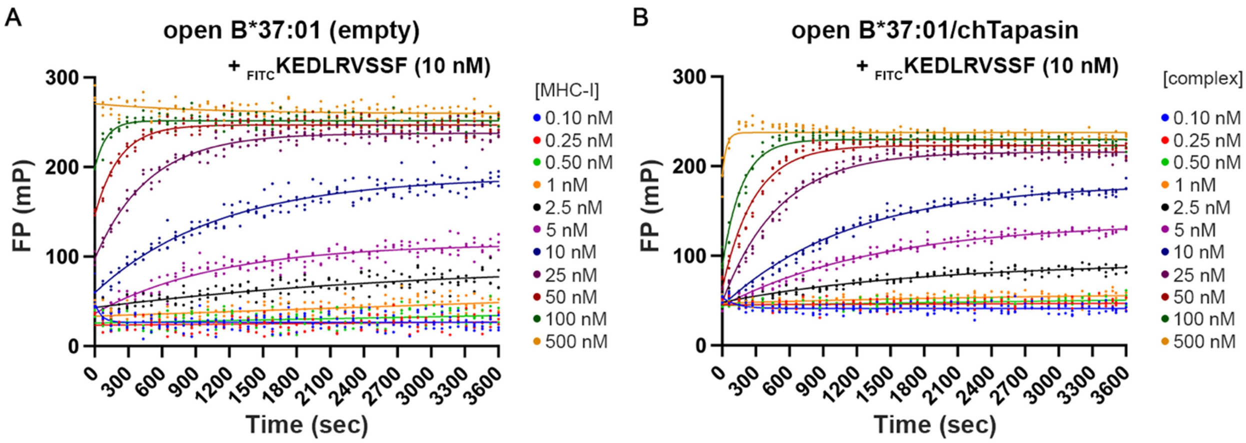

Figure S5. The open B*37:01/chTapasin complex is peptide receptive. Association profile of the fluorophore-conjugated peptide $_{FITC}$KEDLRVSSF (10 nM) to a series of **A.** open, empty B*37:01, and **B.** open B*37:01/chTapasin complex concentrations. The data were fitted to a one-phase association model. Data from n = 3 technical replicates are plotted. FP, fluorescence polarization.

Table S1. Summary of MHC-I contact residues with hTapasin (4) from all HLA allotypes on the SABs. We can distinguish 12 distinct groups (A-L) based on their polymorphic sites (P), which are highlighted in bold in the amino acid sequence.

Group	HLA allotypes	P	**Amino Acid Position** [111, 113, 127, 128, 131, 135, 136, 141, 142, 144, 145, 193, 195, 197, 200, 202, 212, 225, 226, 229, 231, 234, 244, 248]
A	**B*37:01**, B*14:01, B*14:02, B*15:02, B*15:13, B*27:05, B*27:08, B*44:02, B*44:03, B*45:01, B*47:01, B*49:01, B*50:01	-	RYNESAAQIQRPSHTRETQEVRWV
B	B*15:01, B*15:03, B*15:10, B*15:11, B*15:12, B*15:16, B*18:01, B*35:01, B*38:01, B*39:01, B*46:01, B*51:01, B*51:02, B*52:01, B*53:01, B*54:01, B*55:01, B*56:01, B*57:01, B*57:03, B*58:01, B*59:01, B*67:01, B*78:01, B*82:01	Y113H	R**H**NESAAQIQRPSHTRETQEVRWV
C	A*30:01, A*30:02, B*73:01, C*02:02, C*03:02, C*03:03, C*03:04, C*04:01, C*05:01, C*06:02, C*07:02, C*08:01, C*12:03, C*14:02, C*17:01, C*18:02	S131R	RYNE**R**AAQIQRPSHTRETQEVRWV
D	B*07:02, B*08:01, B*40:01, B*40:02, B*40:06, B*41:01, B*42:01, B*48:01, B*81:01, C*15:02	Y113H, S131R	R**H**NE**R**AAQIQRPSHTRETQEVRWV
E	A*01:01, A*03:01, A*11:01, A*11:02, A*36:01, A*80:01	S131R, Q144K	RYNE**R**AAQI**K**RPSHTRETQEVRWV
F	A*25:01, A*26:01, A*29:01, A*29:02, A*31:01, A*32:01, A*33:01, A*33:03, A*34:01, A*34:02, A*43:01, A*66:01, A*66:02, A*74:01	S131R, P193A	RYNE**R**AAQIQR**A**SHTRETQEVRWV
G	C*16:01	S131R, P193L	RYNE**R**AAQIQR**L**SHTRETQEVRWV
H	B*13:01, B*13:02	Y113H, R145L	R**H**NESAAQIQ**L**PSHTRETQEVRWV
I	A*23:01	N127K, S131R	RY**K**E**R**AAQIQRPSHTRETQEVRWV
J	A*24:02, A*24:03	N127K, S131R, Q144K	RY**K**E**R**AAQI**K**RPSHTRETQEVRWV
K	A*02:01, A*02:03, A*02:06,	N127K,	RY**K**E**R**AAQ**TKHA**SHTRETQEVRWV

	A*68:01, A*68:02, A*69:01	S131R, I142T, Q144K, R145H, P193A	
L	C*01:02	V248M	RYNERAAQIQRPSHTRETQEVRW**M**

References

1. Jiang, J., Taylor, D. K., Kim, E. J., Boyd, L. F., Ahmad, J., Mage, M. G., Truong, H. V., Woodward, C. H., Sgourakis, N. G., Cresswell, P., Margulies, D. H., and Natarajan, K. (2022) Structural mechanism of tapasin-mediated MHC-I peptide loading in antigen presentation. *Nat Commun*. **13**, 5470
2. Sievers, F., Wilm, A., Dineen, D., Gibson, T. J., Karplus, K., Li, W., Lopez, R., McWilliam, H., Remmert, M., Söding, J., Thompson, J. D., and Higgins, D. G. (2011) Fast, scalable generation of high-quality protein multiple sequence alignments using Clustal Omega. *Mol Syst Biol*. **7**, 539
3. Robert, X., and Gouet, P. (2014) Deciphering key features in protein structures with the new ENDscript server. *Nucleic Acids Res*. **42**, W320-324
4. Jiang, J., Natarajan, K., Boyd, L. F., Morozov, G. I., Mage, M. G., and Margulies, D. H. (2017) Crystal structure of a TAPBPR–MHC I complex reveals the mechanism of peptide editing in antigen presentation. *Science*. **358**, 1064–1068